

Section 3

Computational studies including new techniques, the effect of varying model resolution, parallel processing

On expansion of analytical functions in ultraspherical polynomials on a sphere.

A.V. Frolov and V.I. Tsvetkov

Hydrometcenter of Russia, Moscow, Russia, tsvetkov@mecom.ru

A new algorithm is suggested for the approximation of an analytical function by double Fourier series on a sphere using a complete set of ultraspherical polynomials as orthogonal basis functions. The Legendre and Chebyshev polynomials of the first and second kinds, which are special cases of the ultraspherical polynomial family, are considered.

The series obtained with the new algorithm uniformly converge in all points of a sphere, including poles. In contrast to traditional spectral series on a sphere, these series explicitly include some additional terms, characterizing an odd (with respect to poles) component of the analytically approximated function.

It is shown that in a small vicinity of poles the resulting double Fourier series becomes simpler because some Fourier terms, responsible for approximation of the odd components of the function, tend to zero in this region.

At the same time, the contribution of the asymmetric (with respect to the pole) components of the approximated function to the Fourier series grows toward the equator and becomes comparable with that of the symmetric components in the equatorial band.

The algorithm was implemented on a computer, and numerical experiments were performed, in which a given scalar continuous analytical function was expanded using spherical harmonics as an orthogonal basis.

The resulting double Fourier series turned out to be longer than the series obtained by any traditional spectral method thus better approximating the given function.

The study was supported by the Russian Foundation for Basic Research (project no. 07-05-13607-ofi_ts).

Forth Order Compact Difference Scheme for Horizontal Block of Forecasting Model.

V.A.Gordin (High School Economics, Hydrometeorological Center of Russia) vagordin@mail.ru,

A.V.Khalyavin (Moscow State University, Hydrometeorological Center of Russia) halyavin@gmail.ru

The typical computational problem in the horizontal block of global forecasting models with implicit or semi-implicit approximation is the following: to restore the horizontal wind by its divergence D and vorticity ζ on the sphere. The problem is solved for every vertical level and on every time step, and therefore its exactness and effectiveness are very important.

Fast Fourier transform $F : f(\varphi, \lambda) \rightarrow \hat{f}(\varphi, m)$ with respect to longitude is a natural approach, but then we obtain a system of ordinary differential equations with variable coefficients and special boundary conditions that both depend on the m . These boundary conditions state that several derivatives of \hat{f} must be equal to zero for original function f to be smooth.

This complex system of differential equations can be separated into 2 independent real systems of differential equations. These systems can be numerically solved by the same algorithm.

We present now a compact scheme with 4-th approximation order for the problem. The equation (all functions here are after Fourier transform) $D = \frac{m}{\sin \varphi} u + v \operatorname{ctg} \varphi + \frac{\partial v}{\partial \varphi}$ is approximated as

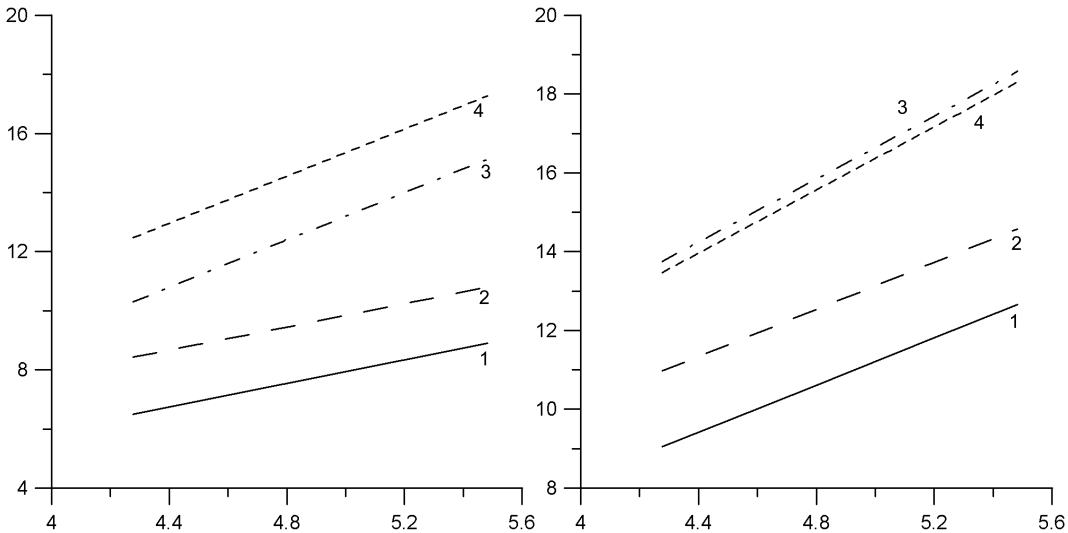
$$\begin{aligned} \frac{1}{6} D_{i-1} + \frac{2}{3} D_i + \frac{1}{6} D_{i+1} &= \frac{m}{6 \sin \varphi_{i-1}} u_{i-1} + \frac{2m}{3 \sin \varphi_i} u_i + \frac{m}{6 \sin \varphi_{i+1}} u_{i+1} + \\ &+ \left[\frac{1}{2h} + \frac{\operatorname{ctg} \varphi_{i+1}}{6} \right] v_{i+1} + \frac{2 \operatorname{ctg} \varphi_i}{3} v_i + \left[-\frac{1}{2h} + \frac{\operatorname{ctg} \varphi_{i-1}}{6} \right] v_{i-1}, \quad i = 2, \dots, N-2 \end{aligned}$$

Similar approximation is used for equation $\zeta = -\frac{m}{\sin \varphi} v - u \operatorname{ctg} \varphi - \frac{\partial u}{\partial \varphi}$. These approximations are not suitable in boundary points due to division by zero. In this case we solve the system of linear equations on coefficients of approximation taking boundary conditions for u , v , D and ζ into account. Then the system of linear equation on u_i and v_i is solved by the sweep method and reverse Fourier transformation is applied.

Our experiments confirmed the announced approximation order. For instance, if

$$\begin{aligned} u &= -\cos \varphi (3 \cos^2 \varphi - 3 \sin^2 \varphi) \sin \lambda - 0.5 \sin \varphi, \quad v = \cos^2 \varphi \cos \lambda, \\ \zeta &= \sin \varphi (16 \sin^2 \varphi - 13) \sin \lambda + \cos \varphi, \quad D = \cos \lambda \sin \varphi \cos \varphi, \end{aligned}$$

Next figures show errors of restoring u and v . Graphics 1 and 2 correspond to the error in u and v when using method from [4]. Graphics 3 and 4 correspond to the error in u and v when using our method. The horizontal axis correspond to logarithm of number of points. The vertical axis correspond to $-\log(\text{error})$.



Left figure shows error in \mathbf{C} metric, while right figure shows errors in \mathbf{L}_2 metric.

References

- [1] Gordin V.A. Mathematical Problems and Methods in Hydrodynamical Weather Forecasting. V.A.Gordin. Gordon & Breach, 2000.
- [2] Gordin V.A. How It Should Be Computed? Mathematical Methods of Computer Assimilation of Information. Moscow Center of Mathematical Continuous Education, 2005 (In Russian).
- [3] V.A.Gordin, A.V.Khalyavin. Projection methods for meteorological fields errors' suppression before derivatives' computation. Meteorology and Hydrology, 2007, N10, 55-65.
- [4] Tolstych M.A. Vorticity-Divergence Semi-Lagrangian Shallow-Water Model of the Sphere Based on Compact Finite Differences, J. Comp.,Phys., 179, 180-200, 2002.

Comparison of simulated diabatic heating profiles between 5km and 1km models in western Japan during the warm season

Teruyuki KATO*

*Meteorological Research Institute / Japan Meteorological Agency, 1-1 Nagamine, Tsukuba, Ibaraki 305-0052, Japan

In the previous report (Kato and Hayashi, 2008), the relation between levels of neutral buoyancy (LNB) thermodynamically estimated from atmospheric condition and cloud-top heights (CTOPs) simulated by a cloud-resolving model with 1 km horizontal grids (1km-CRM) is examined statistically in western Japan during the 2007 Baiu season (June and July). It showed that the deep convection and the warm-rain type convection coexisted in correspondence with upper-level (~ 200 hPa) and middle-level (~ 700 hPa) peaks in LNB appearance frequency obtained statistically from objective analysis data (Kato et al., 2007). In this study, vertical profiles of diabatic heating and cooling are also investigated during the 2008 warm season (from April to August). Moreover, simulated results of a 5km-nonhydrostatic model (5km-NHM) that was used to produce initial and boundary conditions of 1km-CRM are compared with those of 1km-CRM. Numerical models used in this study are the Japan Meteorological Agency NHM (JMANHM, Saito et al., 2007).

At first, the 5km-NHM was nested within JMA mesoscale objective analysis data with a horizontal resolution of 10 km, available 3 hourly (MANAL). Its initial times are 00 UTC, 06 UTC, 12 UTC and 18 UTC of every day, and its integration time is 12 hours (later 6-hour simulated data are used in statics). Next, the 1km-CRM was nested within the output of the 5km-NHM. Its initial time is 3-hour forecast time of the 5km-NHM and hourly simulated data between 4 and 9 forecast hours are used in statics. Accumulated diabatic amounts at every time step are used in this study. In the 1km-CRM, a bulk-type microphysics scheme predicting the specific humidity of cloud water q_c , cloud ice q_{ci} , rainwater q_r , snow q_s , and graupel q_g are used, while a moist convection parameterization scheme (Kain and Fritsch, 1990) is additionally used in the 5km-NHM.

LNB and levels of free convection (LFC) are estimated by a low-level air with the maximum equivalent potential temperature below an 800 hPa level. The cases in which the distance between the originating level of the air and its LFC is longer than 2 km are excluded from statics. CTOPs and cloud-bottom heights (CBTMs) are determined by the threshold values of $q_c + q_{ci} + q_s = 0.01 \text{ g kg}^{-1}$ and $q_c + q_{ci} = 0.1 \text{ g kg}^{-1}$, respectively. Cumulonimbi are defined as the moist convection with rainfall in this study. The following conditions for their judgment are used; 1) the distance from the ground to CTOP > 2 km, 2) the distance from the ground to CBTM < 2.5 km, 3) the distance between CTOP and CBTM > 1 km, and 4) vertically-integrated $q_r + q_s + q_g$ below a 5-km height $\geq 0.1 \text{ mm}$ for CTOP < 8 km. Noted that the location of CTOP may be different from that of CBTM, due to the tilting of cumulonimbi. The difference of vertical scales of cumulonimbi is accepted in this study.

In western Japan, more heavy rainfall events were observed in June 2008, while the Baiu season much earlier ended (~ on 6 July) in comparison with the common year. Moreover, more heavy rainfall events were also observed in August 2008 because of the inflow of humid airs. The upper peak in the LNB appearance rate is very small on the land in June (Fig. 1b), as well as the common year. However, the deep convection, corresponding with the upper peak of 12-13 km in Fig. 2, is more frequently simulated (> 0.3 %) than the LNB appearance rate (< 0.2 %) and could cause heavy rainfall in June. The most part of the deep convection on the land could form over the sea, because the LNB appears at the upper level at a higher rate over the sea.

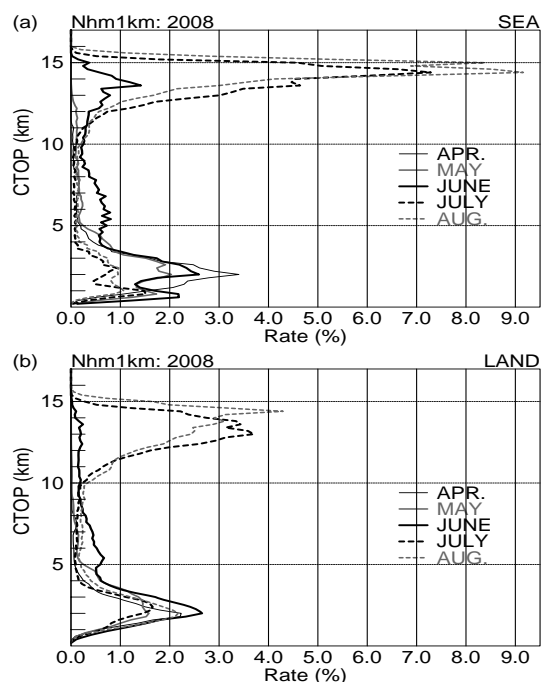


Fig. 1 Vertical profiles of the monthly-averaged LNB appearance rates (a) over the sea and (b) on the land, estimated from 1km-CRM. Each rate is calculated by dividing heights into 80 levels with an interval of 200 m.

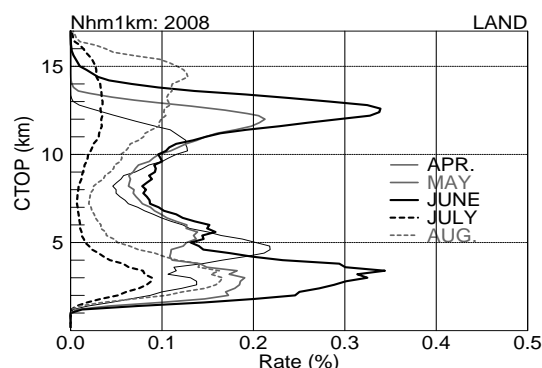


Fig. 2 Same as Fig. 1b, but for the CTOP appearance rate.

The upper peak of CTOPs (Fig. 2) gradually becomes higher associated with the rise of tropopause: from 10 km on April to 15 km on August. However, such a shift in the upper peak of LNB is found only in July and August (Fig. 1b). This suggests that the deep convection form in considerably limited areas around Japan, except during the summer season.

The previous report (Kato and Hayashi, 2007) showed that the 5km-NHM overestimated (underestimated) the appearance rate of the deep convection (the warm-rain type convection), compared with the 1km-CRM. In 2008, the characteristic features of the moist convection simulated by the 1km-CRM are rarely changed. However, the replacement of the boundary conditions of MANAL with the forecast of the JMA global model from that of JMA regional model caused the decrease of the appearance frequency of the moist convection simulated by the 5km-NHM, especially over the sea (not shown). This could be brought from the low-level cold and humid bias, which should be solved in the JMA global model.

Monthly-averaged vertical profiles of the difference of simulated diabatic heating (excluding radiation) and cooling between 5km-NHM and 1km-CRM shows that the difference below a height of 1-4 km is very small over the sea (Fig. 3a), while the 5km-NHM overestimates diabatic heating below a 4 km height on the land (Fig. 3b). Moreover, the 5km-NHM underestimates diabatic heating above a height of 5km both over the sea and on the land. Since these tendencies are also found during the 2007 Baiu season, the difference between 5km-NHM and 1km-CRM could not be caused by the replacement of the boundary conditions of MANAL.

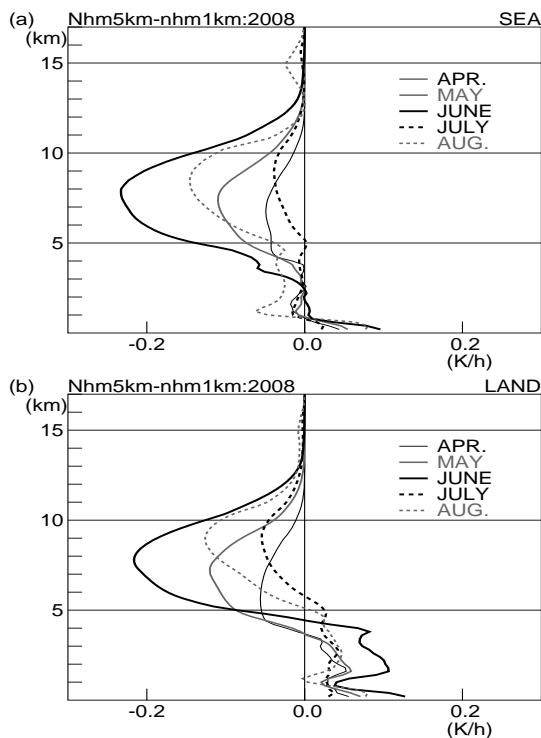


Fig. 3 Monthly-averaged vertical profiles of the difference of simulated diabatic heating and cooling between 5km-NHM and 1km-CRM (a) over the sea and (b) on the land.

The profiles of diabatic heating and cooling in June 2008 are examined in detail. Noted that diabatic cooling is estimated from hourly output, not accumulated at every time step. The 5km-NHM underestimates diabatic cooling, especially at the lower level on the land (see dashed lines in Fig. 4). This is mainly brought from the suppression of raindrop evaporation at a half rate in the 5km-NHM. This rate could be too large, especially on the land.

The profile of diabatic heating simulated by the 1km-CRM has a peak around a height of 1km on the land (Fig. 4b). This is mainly produced by the formation of cloud water due to the terrain-forced updrafts. Moreover, the 5km-NHM underestimates diabatic heating around a height of 7 km. This could be caused by underestimating the upward transportation of water vapor.

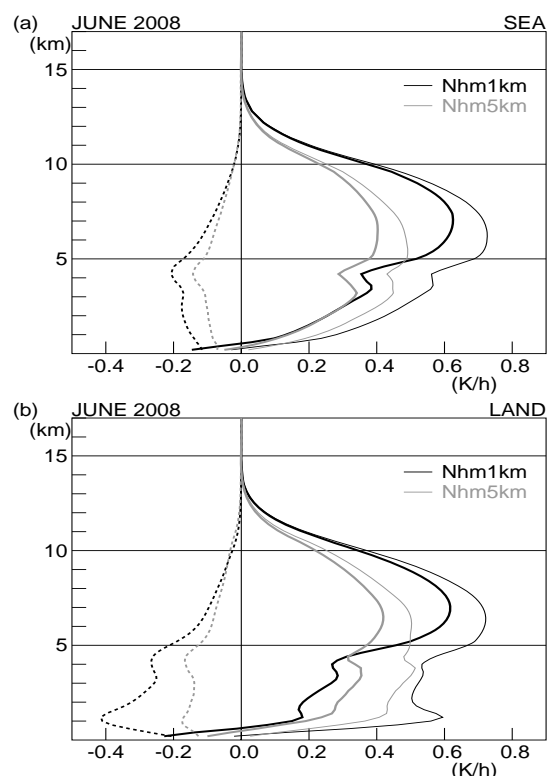


Fig. 4 Vertical profiles of diabatic heating (thin lines) and cooling (dashed lines) simulated by 1km-CRM (black color) and 5km-NHM (gray color) (a) over the sea and (b) on the land, averaged in June 2008. Thick lines represent total of diabatic heating and cooling.

REFERECES

Kain, J. S. and J. M. Fritsch, 1990: A one-dimensional entraining/detraining plume model and its application in convective parameterization. *J. Atmos. Sci.*, **47**, 2784-2802.

Kato, T., S. Hayashi, and M. Yoshizaki, 2007: Statistical study on cloud top heights of cumulonimbi thermodynamically estimated from objective analysis data during the Baiu season. *J. Meteor. Soc. Japan*, **85**, 529-557.

Kato, T. and S. Hayashi, 2008: Problems on the usage of Kain-Fritsch parameterization in a 5km model: Statistical comparison with cloud-top heights of cumulonimbi simulated by a cloud resolving model. *CAS/JSC WGNE Research Activities in Atmospheric and Oceanic Modeling*, **38**, 4.05-4.06.

Saito, K., J. Ishida, K. Aranami, T. Hara, T. Segawa, M. Nareta, and Y. Honda, 2007: Nonhydrostatic atmospheric models and operational development at JMA. *J. Meteor. Soc. Japan*, **85B**, 271-304.

Accurate and Fast Neural Network Full Radiation for the NCEP Climate Forecast System Model

V.M. Krasnopolsky^{1,2} E-mail: Vladimir.Krasnopolsky@noaa.gov,
M. S. Fox-Rabinovitz², Y.-T. Hou¹, S. J. Lord¹, and A. A. Belochitski²

¹Environmental Modeling Center, NCEP/NOAA,

²Earth System Science Interdisciplinary Center, University of Maryland, USA

The approach to calculation of model physics, using accurate and fast neural network (NN) emulations, has been previously proposed, developed and thoroughly tested by the authors for NCAR CAM [Krasnopolsky *et al.* 2005, 2008]. In this study the NN approach has been introduced and tested in the NCEP climate forecast system (CFS) model which is a coupled atmosphere–ocean model with significantly higher resolution, namely for T126 spectral horizontal and high vertical (L = 64 layers) resolutions. Because full model radiation is composed of two, long wave (LW) and short wave (SW), radiation parameterizations which are mappings between their inputs and outputs, NNs can be used to emulate both of these mappings. NNs learn the mappings during the NN training utilizing a training data set which was simulated using the NCEP CFS model run with the original radiation parameterizations.

The model radiation is the most time consuming component of model physics in CFS [e. g. Morcrette *et al.* 2008]. In this study, the NN emulations have been developed and tested for the original RRTM long-wave radiation (LWR) and short wave radiation parameterizations for the CFS model [Mlawer *et al.* 1997].

*Table 1. Statistics estimating the accuracy of heating rates (HRs) (in K/day) calculations and computational performance for NCEP LWR and SWR using NN emulations vs. the original parameterization. Also, layer statistics for the top (bias_H and RMSE_H in K/day) and the bottom (bias_L and RMSE_L in K/day) atmospheric layers are included to illustrate the accuracy of NN emulations in the areas of the increased non-linearity [Morcrette *et al.* 2008].*

NN	Bias (K/day)	RMSE (K/day)	PRMSE (K/day)	Bias _L (K/day)	RMSE _L (K/day)	Bias _H (K/day)	RMSE _H (K/day)	Times Faster
LWR	$2 \cdot 10^{-3}$	0.49	0.39	$6 \cdot 10^{-3}$	0.64	$-9 \cdot 10^{-3}$	0.18	12
SWR	$5 \cdot 10^{-3}$	0.20	0.16	$9 \cdot 10^{-3}$	0.22	$1 \cdot 10^{-2}$	0.21	45

Table 1 shows bulk validation statistics for the accuracy of approximation and computational performance for the developed LWR and SWR NNs emulations. The accuracy of NN emulations is estimated against the original CFS LWR and SWR. For definitions of the error statistics (Bias, RMSE, PRMSE, etc.) see [Krasnopolsky *et al.*, 2005]. PRMSE shown in the Table is the RMSE for the entire profile. For these NN emulations, bias is negligible and RMSE is limited. Obtaining very small NN emulation biases is important for providing non-accumulating errors in the course of model integrations using NN emulations. There is no significant increase in the errors in the areas of the increased non-linearity [Morcrette *et al.* 2008] (the top the bottom layers). The developed highly accurate NN emulations for LWR and SWR, in terms of code-by-code comparison at each model time step when radiation is calculated, are about 12 and 45 times faster than the original/control NCEP CFS LWR and SWR respectively.

The LWR and SWR NN emulations have been validated in 17-year (1990-2007) CFS run. The comparison of time averaged (for the first four seasons and for 17 years) of model prognostic and diagnostic fields shows a close similarity for the parallel runs performed with LWR and SWR NN emulations and with the original LWR and SWR (the control run). The difference between 17-year mean SST fields (NN – control runs) is presented in Fig. 1 (left

panel). The difference is close to zero and does not exceed ± 0.5 K. The difference between 17-year mean precipitation rate fields (NN – control runs) is presented in Fig. 1 (right panel). The difference is small and does not exceed ± 1 mm/day except for a few spots in the tropics where it is within ± 3 mm/day. Similar results are obtained for other prognostic and diagnostics fields [Krasnopolsky et al. 2009].

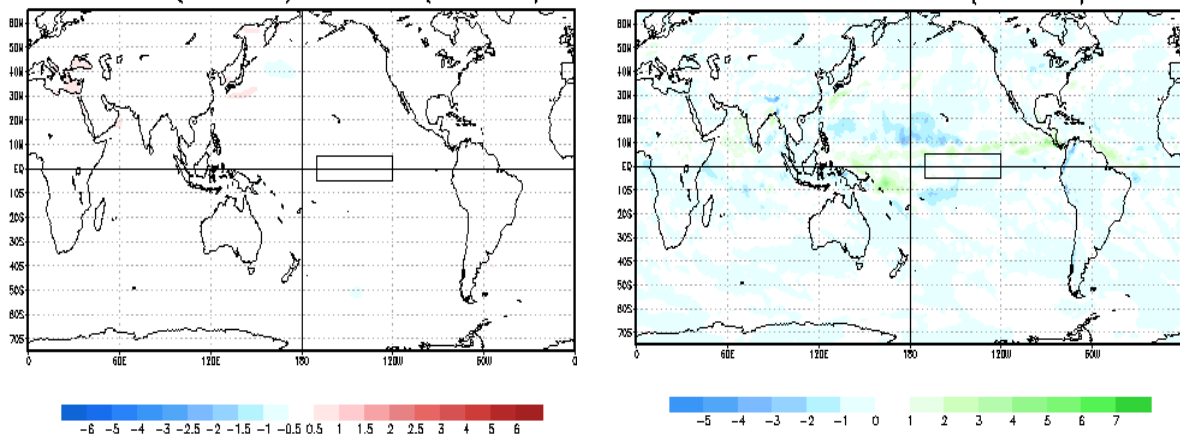


Fig. 1 The time mean (1990-2006) statistics for winter for the difference between the full radiation NN run and the control. The left panels: the SST statistics in K. The right panels: the precipitation rate statistics in mm/day.

In this study we demonstrated that our NN emulation approach provides a sufficient accuracy and speed of radiation calculations to be used in high resolution state-of-the-art coupled models like NCEP CFS and that it is significantly less dependent (in terms of both the accuracy and speed) on the increase of the vertical resolution than “NeuroFlux” for which at vertical resolution of 60 layers and more, both accuracy and rapidity could not be kept at once [Morcrette et al. 2008]. The further steps will include refinement of NN emulations for the CFS model, introduction of the concept of a compound parameterization including a quality control procedure, and the NN ensemble approach.

Acknowledgments The authors would like to thank Drs. H.-L. Pan, S. Saha, S. Moorthi, and M. Iredell for their useful consultations and discussions. The research is supported by the NOAA CPO CDEP CTB (Climate Test Bed) grant NA06OAR4310047.

References

- Krasnopolsky, V.M., M.S. Fox-Rabinovitz, and D.V. Chalikov, 2005: “Fast and Accurate Neural Network Approximation of Long Wave Radiation in a Climate Model”, *Monthly Weather Review*, vol. 133, No. 5, pp. 1370-1383.
- Krasnopolsky, V. M., M.S. Fox-Rabinovitz, and A. A. Belochitski, 2008: “Decadal Climate Simulations Using Accurate and Fast Neural Network Emulation of Full, Long- and Short Wave, Radiation, *Monthly Weather Review*, 136 3683–3695, doi: 10.1175/2008MWR2385.1.
- Mlawer, E.J., S.J. Taubman, P.D. Brown, M.J. Iacono, and S.A. Clough, 1997: “Radiative transfer for inhomogeneous atmospheres: RRTM, a validated correlated-k model for the longwave, *J. Geophys. Res.*, 102, D14, 16,663-16,682
- Morcrette, J.-J., G. Mozdzynski and M. Leutbecher, 2008: “A reduced radiation grid for the ECMWF Integrated Forecasting System”, *Monthly Weather Review*, 136, 4760-4772, doi: 10.1175/2008MWR2590.1
- Krasnopolsky, V.M, M.S. Fox-Rabinovitz, S. J. Lord, Y. T. Hou, A.A. Belochitski, 2009: “Accurate and Fast Neural Network Emulations of Model Radiation for the High Resolution, Coupled NCEP Climate Forecast System: Climate Simulations and Seasonal Predictions”, *Monthly Weather Review*, submitted.

Research on Computational Techniques for JMA's NWP Models

Kensuke Takenouchi, Shintaro Yokoi, Chiashi Muroi, Junichi Ishida and Kohei Aranami
Numerical Prediction Division, Japan Meteorological Agency,
1-3-4 Otemachi, Chiyoda-ku, Tokyo 100-8122, Japan
E-mail: k.takenouchi@met.kishou.go.jp

1. Introduction

The Japan Meteorological Agency (JMA) is currently implementing a comprehensive program of assessment and research on computational techniques.

Recent trends regarding HPCs (high-performance computers) indicate that cluster machines have accounted for a large share of the market in the last decade.

This report describes the performance of JMA's NWP models on two kinds of cluster machines and the effectiveness of computational techniques implemented on them.

2. TSUBAME and SCS8

Table 1 shows the specifications of TSUBAME (a computing system at the Tokyo Institute of Technology) and SCS8 (JMA's eighth operational supercomputer system). TSUBAME is composed of 655 nodes (Sun Fire X4600), and has more memory per node than ordinary PC clusters. SCS8 is composed of 210 nodes (Hitachi SR11000), and represents a typical SMP HPC.

Table 1. Machine specifications

Machine name	TSUBAME	SCS8
Total performance	85 TFlops	27.5 TFlops
Number of nodes	655 (16 CPU/node)	210 (16 CPU/node)
Amount of memory	32 GB/node	64 GB/node
Memory bandwidth	6.4 GB/s	15 GB/s
Speed between nodes	Two-way, 2 GB/s	Two-way, 16 GB/s
CPU	AMD Opteron 880 (2.4 GHz), 885 (2.6 GHz)	POWER5+ (1.9 GHz, 2.1 GHz)

3. Scalability and profiles

The scalability and profiles of JMA's Global Spectrum Model (GSM; for details, see <http://www.jma.go.jp/jma/jma-eng/jma-center/nwp/nwp-top.htm>) and its NonHydrostatic regional Model (NHM, Saito et al., 2007) were measured using TSUBAME and SCS8. Table 2 shows the settings of the experiments, while Figs. 1 and 2 show the scalability and profiles, respectively.

The scalability of both the GSM and the NHM on TSUBAME are close to the ideal lines, while the performance of the GSM on SCS8 hardly

increases over about 32 processes. This does not necessarily signify that TSUBAME is better than SCS8. In fact, the total execution time with eight nodes on TSUBAME is five times longer for the GSM and ten times longer for the NHM than on SCS8, although the theoretical peak performance per node of TSUBAME is almost the same as that of SR11000. Considering that the memory bandwidth of TSUBAME is lower than that of SCS8, the better scalability on TSUBAME is considered to be due to the decrease in memory load per process resulting from the increased number of nodes.

From Fig. 2, it can be seen that the rates of communication time on the GSM and NHM increase with higher numbers of nodes, which indicates that measures to reduce communication time are necessary for both models.

Table 2. Experimental settings of models

Model	GSM	NHM
Resolution	TL319	2 km
Number of grid points	640 x 320 x 60	800 x 550 x 60
Number of calculation steps (forecast period)	72 (one day)	60 (ten minutes)
Number of processes	1 per node	1 per node
Number of threads	16 per process	16 per process
SMP	OpenMP	OpenMP

4. Computational technique

(i) Parallelization of calculation and communication

The parallelization of calculation and communication was examined as a way of reducing the total execution times of the models.

Two cases of such parallelization are shown in Fig 3. One is parallelization in one process, and the other is parallelization with threads. Research has shown that these parallelization techniques generally reduce the total execution time to some extent. However, the amount of reduction depends on the kind of machine, and the effects in total models are unclear. Additionally, extensive modification of model codes is necessary to enable these techniques to be applied to JMA's NWP models. As a result, these parallelization methods have not been applied,

and remain under research at JMA.

(ii) kij-ordering

In JMA's NWP models (such as the NHM), variable arrays are set sequentially in the order of x, y, z (ijk-ordering: a(i, j, k)). However, setting them sequentially in the order of z, x, y (kij-ordering: a(k, i, j)) works more effectively to increase speed in terms of cache tuning, for example, in the case of calculation in the Z direction (M. Ashworth et al., 2001; J. Michalakes et al., 2001). The effectiveness of kij-ordering is to be investigated in the development of a new dynamical core for nonhydrostatic model.

Reference

Saito, K., J. Ishida, K. Aranami, T. Hara, T. Segawa, M. Narita, and Y. Honda, 2007:

Nonhydrostatic Atmospheric Models and Operational Development at JMA. *J. Meteor. Soc. Japan*, 85B, 271–304.

Ashworth M., R. Proctor, J. T. Holt, J. I. Allen, and J. C. Blackford, 2001: Coupled marine ecosystem modelling on high performance computers. *Developments in Teracomputing: Proceedings of the Ninth ECMWF Workshop on the Use of High Performance Computing in Meteorology*, W. Zwiefelhofer and N. Kreitz, Eds., World Scientific, 150–163.

Michalakes, J., R. Loft, A. Bourgeois, 2001 : "Performance-Portability and the Weather Research and Forecast Model" in on-line proceedings of the HPC Asia 2001 conference, Gold Coast, Queensland, Australia, September 24-28.

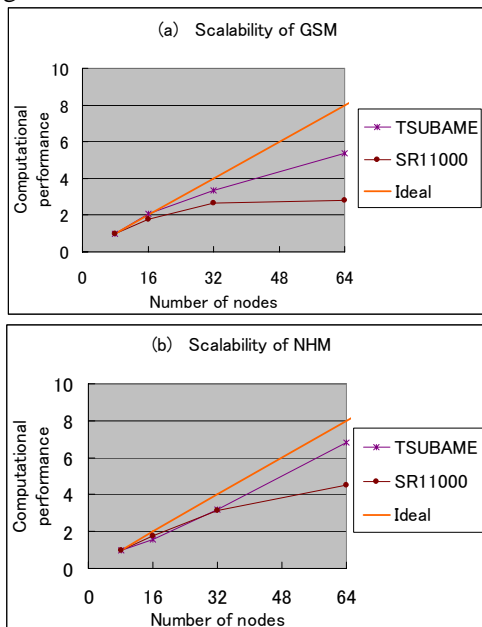


Fig. 1. Scalability of JMA's NWP models based on eight-node performance. (a) GSM, (b) NHM (1 process/node, 16 threads/process)

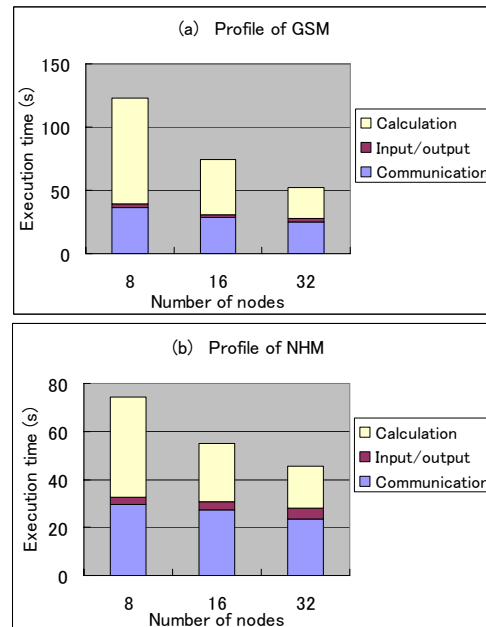


Fig. 2. Profiles of JMA's NWP models on SCS8. (a) GSM, (b) NHM (1 process/node, 16 threads/process)

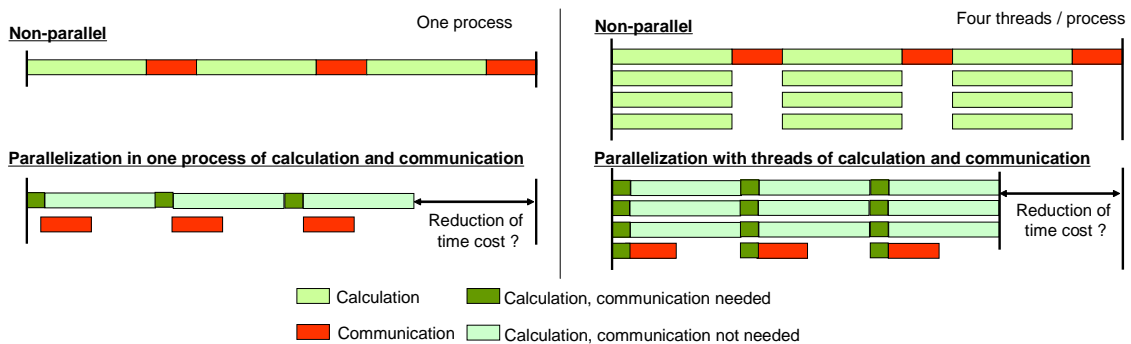


Fig. 3. Examples showing parallelization of calculation and communication. Left: parallelization in one process. Right: parallelization with four threads.